Amplification of advanced modulation formats with a semiconductor optical amplifier cascade

S. Koenig,[1,2] R. Bonk,[3] H. Schmuck,[3] W. Poehlmann,[3] Th. Pfeiffer,[3] C. Koos,[1] W. Freude,[1,*] and J. Leuthold[1,4]

[1]*Karlsruhe Institute of Technology (KIT), Engesserstraße. 5, 76131 Karlsruhe, Germany*
[2]*Now with: Infinera Corporation, 140 Caspian Ct, Sunnyvale, CA 94089, USA*
[3]*Alcatel-Lucent Bell Labs Germany, Lorenzstraße 10, 70435 Stuttgart, Germany*
[4]*Now with: Swiss Federal Institute of Technology (ETH) Zurich, Gloriastraße 35, 8092 Zurich, Switzerland*
[*]*w.freude@kit.edu*

Abstract: The convergence of optical metro networks and access networks extends the area of network coverage, and therefore requires the use of optical amplifiers. For this purpose, semiconductor optical amplifiers (SOA) would be attractive, because they are broadband, can be centered between 1250 nm and 1600 nm, and because they are cheap in production and operation. We show that signals encoded with advanced modulation formats such as BPSK, QPSK, 8PSK, and 16QAM can be amplified by a cascade of at least four SOAs. This enables high-capacity paths with a capacity in the order of Tbit/s for converged metro-access networks.

OCIS codes: (250.5980) Semiconductor optical amplifiers; (060.1660) Coherent communications.

References and links

1. D. R. Zimmerman and L. H. Spiekman, "Amplifiers for the masses: EDFA, EDWA, and SOA amplets for metro and access applications," J. Lightwave Technol. **22**(1), 63–70 (2004).
2. H. Schmuck, R. Bonk, W. Poehlmann, C. Haslach, W. Kuebart, D. Karnick, J. Meyer, D. Fritzsche, E. Weis, J. Becker, W. Freude, and Th. Pfeiffer, "Demonstration of an SOA-assisted open metro-access infrastructure for heterogeneous services," Opt. Express **22**(1), 737–748 (2014).
3. S. Koenig, R. Bonk, R. M. Schmogrow, A. Josten, D. Karnick, H. Schmuck, W. Poehlmann, Th. Pfeiffer, C. Koos, W. Freude, and J. Leuthold, "Cascade of 4 SOAs with 448 Gbit/s (224 Gbit/s) dual channel dual polarization 16QAM (QPSK) for high-capacity business paths in converged metro-access Networks," *Optical Fiber Communication Conference (OFC)*, Anaheim (CA), USA, (2013), paper OTh4A.3.
4. Th. Pfeiffer, "New avenues of revenues - Open access and infrastructure virtualization," *Optical Fiber Communication Conference (OFC)*, Los Angeles (CA), USA, (2012), paper NTh4E.1, *http://ieeexplore.ieee.org/xpls/abs_all.jsp?arnumber=6476310*.
5. J. Leuthold, R. Ryf, D. N. Maywar, S. Cabot, J. Jaques, and S. S. Patel, "Nonblocking all-optical cross connect based on regenerative all-optical wavelength converter in a transparent demonstration over 42 nodes and 16800 km," J. Lightwave Technol. **21**(11), 2863–2870 (2003).
6. J. Wang, A. Maitra, C. G. Poulton, W. Freude, and J. Leuthold, "Temporal dynamics of the alpha factor in semiconductor optical amplifiers," J. Lightwave Technol. **25**(3), 891–900 (2007).
7. G. Contestabile, "All optical processing in QD-SOAs," *Optical Fiber Communication Conference (OFC)*, San Francisco (CA), USA (2014), paper W4F.6.
8. W. Freude, R. Bonk, T. Vallaitis, A. Marculescu, A. Kapoor, E. K. Sharma, C. Meuer, D. Bimberg, R. Brenot, F. Lelarge, G.-H. Duan, C. Koos, and J. Leuthold, "Linear and nonlinear semiconductor optical amplifiers," *12th International Conference on Transparent Optical Networks (ICTON),* Munich, Germany, (2010), paper We.D4.1.
9. J. Leuthold, R. Bonk, T. Vallaitis, A. Marculescu, W. Freude, C. Meuer, D. Bimberg, R. Brenot, F. Lelarge, and G.-H. Duan, "Linear and nonlinear semiconductor optical amplifiers," *Optical Fiber Communication Conference (OFC)*, San Diego (CA), USA, (2010), paper OThI3.
10. Th. Pfeiffer, "Converged heterogeneous optical metro-access networks," *36th European Conference on Optical Communication (ECOC)*, Torino, Italy, (2010), paper Tu.5.B.1.
11. R. Bonk, T. Vallaitis, J. Guetlein, C. Meuer, H. Schmeckebier, D. Bimberg, C. Koos, W. Freude, and J. Leuthold, "The input power dynamic range of a semiconductor optical amplifier and its relevance for access network applications," IEEE Photonics J. **3**(6), 1039–1053 (2011).
12. R. J. Manning, D. A. O. Davies, and J. K. Lucek, "Recovery rates in semiconductor laser amplifiers: optical and electrical bias dependencies," Electron. Lett. **30**(15), 1233–1235 (1994).

#211942 - $15.00 USD Received 12 May 2014; revised 29 Jun 2014; accepted 30 Jun 2014; published 16 Jul 2014

13. D. Wolfson, S. L. Danielsen, C. Joergensen, B. Mikkelsen, and K. E. Stubkjaer, "Detailed theoretical investigation of the input power dynamic range for gain-clamped semiconductor optical amplifier gates at 10 Gb/s," IEEE Photon. Technol. Lett. **10**(9), 1241–1243 (1998).
14. D. A. Francis, S. P. DiJaili, and J. D. Walker, "A single-chip linear optical amplifier," *in Optical Fiber Communication Conference, 2001 OSA Technical Digest Series (Optical Society of America, 2001),* paper PD13, *http://www.opticsinfobase.org/abstract.cfm?URI=OFC-2001-PD13*.
15. C. Michie, A. E. Kelly, I. Armstrong, I. Andonovic, and C. Tombling, "An adjustable gain-clamped semiconductor optical amplifier (AGC-SOA)," J. Lightwave Technol. **25**(6), 1466–1473 (2007),.
16. H. N. Tan, M. Matsuura, and N. Kishi, "Enhancement of input power dynamic range for multiwavelength amplification and optical signal processing in a semiconductor optical amplifier using holding beam effect," J. Lightwave Technol. **28**(17), 2593–2602 (2010).
17. J. Yu and P. Jeppesen, "Increasing input power dynamic range of SOA by shifting the transparent wavelength of tunable optical filter," J. Lightwave Technol. **19**(9), 1316–1325 (2001).
18. J. Leuthold, D. M. Marom, S. Cabot, J. J. Jaques, R. Ryf, and C. R. Giles, "All-optical wavelength conversion using a pulse reformatting optical filter," J. Lightwave Technol. **22**(1), 186–192 (2004).
19. M. Sauer and J. Hurley, "Experimental 43 Gb/s NRZ and DPSK performance comparison for systems with up to 8 concatenated SOAs," in *Conference on Lasers and Electro-Optics/Quantum Electronics and Laser Science Conference and Photonic Applications Systems Technologies,* Technical Digest (CD) (Optical Society of America, 2006), paper CThY2, *http://www.opticsinfobase.org/abstract.cfm?URI=CLEO-2006-CThY2*.
20. E. Ciaramella, A. D'Errico, and V. Donzella, "Using semiconductor-optical amplifiers with constant Envelope WDM Signals," IEEE J. Quantum Electron. **44**(5), 403–409 (2008).
21. J. D. Downie and J. Hurley, "Effects of dispersion on SOA nonlinear impairments with DPSK signals," in *Proc. of 21st Annual Meeting of the IEEE Lasers and Electro-Optics Society, LEOS 2008,* paper WX3.
22. P. S. Cho, Y. Achiam, G. Levy-Yurista, M. Margalit, Y. Gross, and J. B. Khurgin, "Investigation of SOA nonlinearities on the amplification of high spectral efficiency signals," *in Optical Fiber Communication Conference, OSA Technical Digest (CD) (Optical Society of America, 2004),* paper MF70, *http://www.opticsinfobase.org/abstract.cfm?URI=OFC-2004-MF70*.
23. X. Wei, Y. Su, X. Liu, J. Leuthold, and S. Chandrasekhar, "10-Gb/s RZ-DPSK transmitter using a saturated SOA as a power booster and limiting amplifier," IEEE Photon. Technol. Lett. **16**, 1582–1584 (1998).
24. H. Takeda, N. Hashimoto, T. Akashi, H. Narusawa, K. Matsui, K. Mori, S. Tanaka, and K. Morito, "Wide range over 20 dB output power control using semiconductor optical amplifier for 43.1 Gbps RZ-DQPSK signal," *35th European Conference on Optical Communication (ECOC 2009),* paper 5.3.4, *http://ieeexplore.ieee.org/stamp/stamp.jsp?tp=&arnumber=5287100&isnumber=5286960*.
25. T. Vallaitis, R. Bonk, J. Guetlein, D. Hillerkuss, J. Li, R. Brenot, F. Lelarge, G.-H. Duan, W. Freude, and J. Leuthold, "Quantum dot SOA input power dynamic range improvement for differential-phase encoded signals," Opt. Express **18**(6), 6270–6276 (2010), doi:10.1364/OE.18.006270.
26. R. Bonk, G. Huber, T. Vallaitis, S. Koenig, R. Schmogrow, D. Hillerkuss, R. Brenot, F. Lelarge, G. H. Duan, S. Sygletos, C. Koos, W. Freude, and J. Leuthold, "Linear semiconductor optical amplifiers for amplification of advanced modulation formats," Opt. Express **20**(9), 9657–9672 (2012).
27. R. Bonk, G. Huber, T. Vallaitis, R. Schmogrow, D. Hillerkuss, C. Koos, W. Freude, and J. Leuthold, "Impact of alfa-factor on SOA dynamic range for 20 GBd BPSK, QPSK and 16-QAM signals," in *Optical Fiber Communication Conference, OSA Technical Digest (CD) (Optical Society of America, 2011),* paper OML4, *http://www.opticsinfobase.org/abstract.cfm?URI=OFC-2011-OML4*.
28. N. Kamitani, Y. Yoshida, and K. Kitayama, "Experimental Study on Impact of SOA Nonlinear Phase Noise in 40Gbps Coherent 16QAM Transmissions," *European Conference and Exhibition on Optical Communication (ECOC)*, Amsterdam, (2012), paper P1.04.
29. S. Lange, G. Contestabile, Y. Yoshida, and K. Kitayama, "Phase-transparent Amplification of 16 QAM Signals in a QD-SOA," IEEE Photon. Technol. Lett. **25**(24), 2486–2489 (2013).
30. S. Lange, Y. Yoshida, and K. Kitayama, "A Low-complexity Digital Pre-compensation of SOA Induced Phase Distortion in Coherent QAM Transmissions," *Optical Fiber Communication Conference (OFC)*, Anaheim, California, (2013), paper OTh3C.7, *http://ieeexplore.ieee.org/xpls/abs_all.jsp?arnumber=6532893*.
31. S. Amiralizadeh, A. T. Nguyen, P. Chul Soo, A. Ghazisaeidi, and L. A. Rusch, "Experimental validation of digital filter back-propagation to suppress SOA-induced nonlinearities in 16-QAM," *Optical Fiber Communication Conference (OFC)*, (2013), paper OM2B.2, *http://ieeexplore.ieee.org/xpls/abs_all.jsp?arnumber=6532738*.
32. L. H. Spiekman, J. M. Wiesenfeld, A. H. Gnauck, L. D. Garrett, G. N. Van den Hoven, T. Van Dongen, M. J. H. Sander-Jochem, and J. J. M. Binsma, "8 x 10 Gb/s DWDM transmission over 240 km of standard fiber using a cascade of semiconductor optical amplifiers," IEEE Photon. Technol. Lett. **12**(8), 1082–1084 (2000).
33. N. Antoniades, K. C. Reichmann, P. P. Iannone, and A. M. Levine, "Engineering methodology for the use of SOAs and CWDM transmission in the metro network environment," *Optical Fiber Communication Conference (OFC)*, Anaheim (CA), USA, 2006, paper OTuG6, *http://www.opticsinfobase.org/abstract.cfm?URI=OFC-2006-OTuG6*.
34. S. Liu, K. A. Williams, T. Lin, M. G. Thompson, C. K. Yow, A. Wonfor, R. V. Penty, I. H. White, F. Hopfer, M. Lämmlin, and D. Bimberg, "Cascaded performance of quantum dot semiconductor optical amplifier in a recirculating loop," *Conference on Lasers and Electro-Optics (CLEO) and on Quantum Electronics and Laser Science (QELS)*, 2006, paper CTuM4, *http://ieeexplore.ieee.org/xpls/abs_all.jsp?arnumber=4628243&tag=1*.

#211942 - $15.00 USD Received 12 May 2014; revised 29 Jun 2014; accepted 30 Jun 2014; published 16 Jul 2014

35. R. Schmogrow, D. Hillerkuss, M. Dreschmann, M. Huebner, M. Winter, J. Meyer, B. Nebendahl, C. Koos, J. Becker, W. Freude, and J. Leuthold, "Real-time software-defined multiformat transmitter generating 64QAM at 28 GBd," IEEE Photon. Technol. Lett. **22**(21), 1601–1603 (2010).
36. R. Schmogrow, B. Nebendahl, M. Winter, A. Josten, D. Hillerkuss, S. Koenig, J. Meyer, M. Dreschmann, M. Huebner, C. Koos, J. Becker, W. Freude, and J. Leuthold, "Error vector magnitude as a performance measure for advanced modulation formats," IEEE Photon. Technol. Lett. **24**, 61–63 (2012). (Correction: ibid. **24**, 2198 (2012)).

1. Introduction

Semiconductor optical amplifiers (SOA) for linear amplification of optical fields have gained interest as in-line amplifiers in optical communication networks [1–4]. For this purpose they are designed to have large saturation powers and a moderate gain. In this respect, these so-called *linear* SOA differ from *nonlinear* SOA, which are designed for small saturation powers and a large gain, and are used mainly for optical signal processing such as all-optical switching, regeneration, or wavelength conversion [5–7]. Some design guidelines for tailoring the saturation power of SOAs based on important physical parameters such as gain, material gain coefficient, differential gain, field confinement factor, carrier concentration, effective carrier lifetime, longitudinal SOA extension, and doping profile can be found in [8,9].

Linear SOAs might become an attractive alternative to erbium-doped fiber amplifiers (EDFA), because SOAs are considered cost-efficient devices offering a broader gain spectrum (up to 100 nm) compared to EDFAs (typically 30 nm to 70 nm). This means that SOAs with fewer different center wavelengths are needed compared to EDFAs. In addition, the gain spectrum of SOAs can be centered at virtually any wavelength in a 10 THz window between 1250 nm and 1600 nm. Thus, SOAs are available for the O-band (1300 nm), a range that could otherwise be covered by praseodymium-doped fiber amplifiers only, which are still relatively expensive. The possibility of integrating SOAs in photonic integrated circuits, their small form factor, and their small power consumption enable systems with high component density leading to lower installation and operational expenses.

In the near future, optical metro networks and access networks will converge more and more, i.e., both the metro network infrastructure and the last mile infrastructure merge to one metro-access infrastructure [2, 10]. This converged metro-access network approach offers a large fiber-based capacity in a wide area. Figure 1 depicts a converged metro-access ring network scenario. With a feeder ring circumference of 30 to 60 km and a coverage area of about 300 km^2, this network serves a large number of subscribers (>100,000) in urban areas of mid-sized European cities. Such a network architecture offers virtually unlimited bandwidth for all kind of customers and infrastructures such as gigabit passive optical networks (GPON), fiber-to-the-x (FTTx with x = B, H for building, home), radio backhauling, and also high-capacity paths between enterprise customers, data centers, and large institutions such as universities or research centers. A high-capacity path from one enterprise to another offers, e.g., a 100 Gbit/s capacity which could be provided by the use of advanced modulation formats and/or polarization multiplexing such as 25 GBd DP-QPSK (dual polarization quadrature phase-shift keying) or 25 GBd 16QAM (quadrature amplitude modulation).

In the following, we first discuss the application of linear SOAs in a metro-access ring network, then explain an experimental setup with a linear SOA cascade for amplifying signals encoded with advanced modulation formats, and finally provide detailed experimental results.

2. Cascaded SOAs in converged metro-access networks

Previous SOA studies mainly focused on identifying the optimum operating conditions of a *stand-alone* SOA, and on increasing its linear operation range. These aspects and related issues have been extensively investigated for on-off-keying (OOK) data signals [11–18] as well as for PSK formats such as differential (D) PSK [19–23] and DQPSK [24,25]. With the advent of coherent optical data communications, SOAs are required to tolerate signals encoded with advanced modulation formats such as QAM, which combines aspects of both amplitude-shift keying (ASK) and PSK formats. Some results have been already reported on the amplification of QAM signals by a stand-alone SOA [26–29], and different schemes for pre-

#211942 - $15.00 USD Received 12 May 2014; revised 29 Jun 2014; accepted 30 Jun 2014; published 16 Jul 2014

compensating [30] and post-compensating [31] SOA-induced nonlinearities in coherent QAM transmission systems have been proposed.

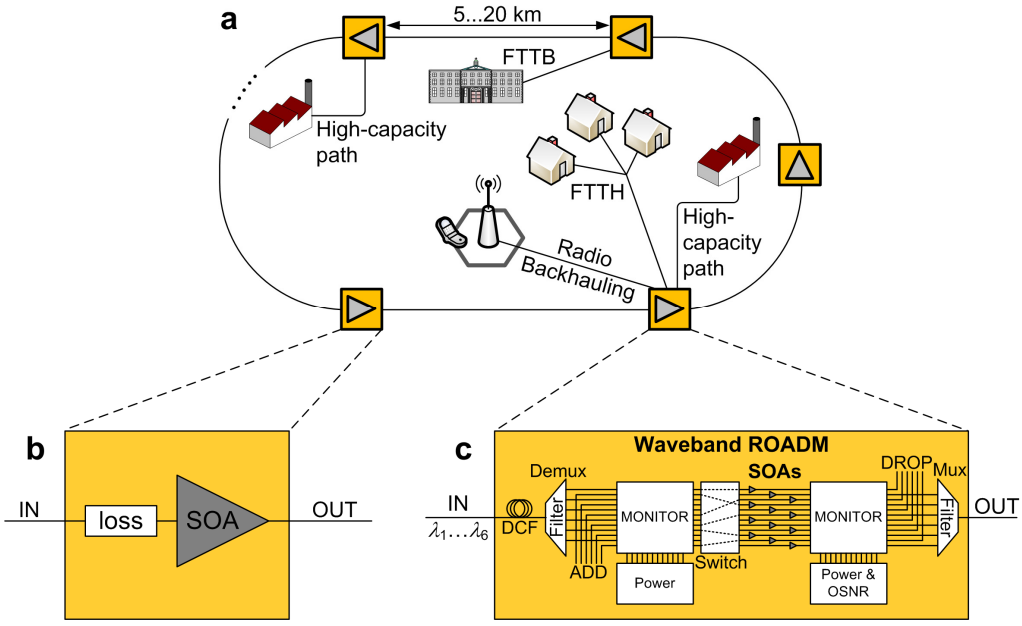

Fig. 1. Converged metro-access ring network scenario. (a) Infrastructures such as fiber-to-the-x (FTTx with x = B, H for building, home), radio backhauling, or high-capacity paths are supported. (b) SOAs along the ring compensate losses in the network so that a cascade of several SOAs results. (c) SOAs may be located in waveband ROADMs which provide data switching every 5 to 20 km. SOA = semiconductor optical amplifier, CWDM = coarse wavelength division multiplexing, ROADM = reconfigurable optical add-drop multiplexer, DCF = dispersion compensating fiber, Mux = multiplexer, Demux = de-multiplexer, MONITOR = monitor tap, OSNR = optical signal-to-noise-ratio.

However, in many network scenarios a basic requirement is the capability of *cascading* several amplifiers. As an example, Fig. 1(a) depicts a ring network where SOAs are used to compensate the losses along the ring. Figure 1(b) illustrates a simplified model comprising an SOA that compensates any kind of loss in the network. In a more detailed view as depicted in Fig. 1(c), the SOA may be part of a reconfigurable optical add-drop multiplexer (ROADM) that makes the network versatile and supports several wavelength bands (λ_1 to λ_6). The spectral width of a wavelength band may range from a few nanometers to a coarse wavelength division multiplexing (CWDM) 20 nm channel grid. Each band comprises several subchannels where data are transmitted employing different multiplexing techniques, modulation formats, and channel powers. For each band, one dedicated SOA compensates for the ROADM losses and for the transmission losses along the ring. Yet, in both cases a cascade of SOAs results.

Evidently, to support large data rates beyond 100 Gbit/s, the SOA cascade must cope with advanced modulation formats and multi-channel operation. Up to now, cascaded SOAs have only been examined for OOK [32–34] and for DPSK [19]. Virtually nothing is known about the practicality of an SOA cascade scenario with advanced modulation formats such as 8PSK as well as 16QAM and DP signals.

In this paper, we mimic a converged metro-access ring network scenario with a cascade of four commercially available linear SOAs. We investigate single λ-channel and dual λ-channel operation using single polarization (SP) and DP 28 GBd/channel binary (B)PSK, QPSK, 8PSK and 16QAM signals. This enables the transmission of aggregate data capacities of up to 448 Gbit/s. We evaluate the limiting factors, the achievable input power dynamic range (IPDR), polarization dependent issues, and the optimum SOA operating conditions. For the

#211942 - $15.00 USD Received 12 May 2014; revised 29 Jun 2014; accepted 30 Jun 2014; published 16 Jul 2014

single λ-channel SP QPSK signal we also investigate the impact of different filter bandwidths (17 nm CWDM-filter, 2 nm, and no filter) after each SOA, as it influences on the achievable IPDR and the number of cascadable SOAs. To the best of our knowledge, this is the first detailed study of the performance of cascaded SOAs transmitting signals with advanced modulation formats.

The optimum SOA input power is found 11 dB below the 1 dB saturation input power, showing that linearity requirements for the SOAs are high and that the operating conditions of the network are primarily dictated by the SOA. When employing a 17 nm CWDM filter after each SOA, we observe a large IPDR of 20 dB for QPSK after the fourth SOA. For 8PSK, good IPDR values of 8…12 dB are obtained, and for 16QAM an IPDR of still 4…8 dB is achieved. For the single λ-channel SP QPSK signal, the use of a 2 nm filter bandwidth increases the IPDR by about 4 dB compared to the case with CWDM filter. However, without any filter after each SOA, the IPDR after the fourth SOA decreases by almost 10 dB.

3. Experimental setup

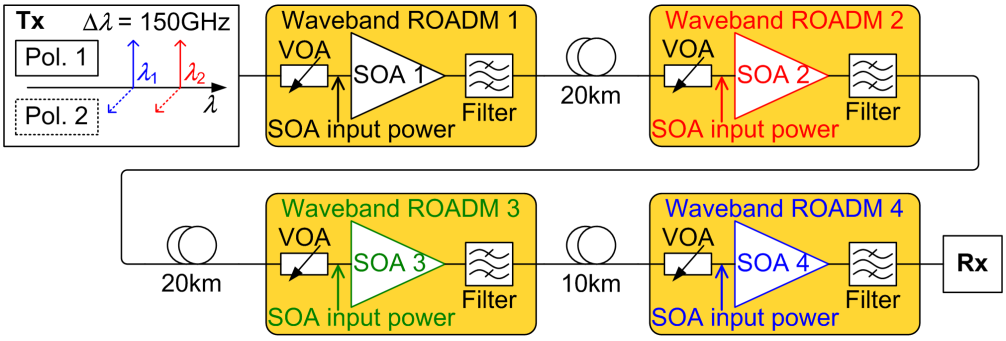

Fig. 2. Experimental setup with four cascaded waveband ROADMs to mimic a high-capacity path in a converged metro-access network (see Fig. 1). Identical SOAs in each waveband ROADM amplify the data signal which is then filtered. The total signal power into the first SOA is adjusted by the first VOA. All other VOAs are adjusted such that all SOAs have equal input power for a 0 dB net gain between subsequent SOA inputs.

Our experimental setup (Fig. 2) mimics a high-capacity path over up to four cascaded waveband ROADMs within the scenario of Fig. 1. It comprises a software-defined multi-format transmitter (Tx) [35] encoding decorrelated data onto one or two optical carrier(s) at 1550.92 nm and 1549.72 nm (λ-channel spacing 150 GHz), and on one or two decorrelated polarization channels. The Tx symbol rate is 28 GBd. A coherent receiver (Rx, Agilent N4391 optical modulation analyzer, OMA) processes the signals offline and provides dispersion compensation. For single λ-channel (dual polarization) operation, the bitrates are 28 Gbit/s (56 Gbit/s) BPSK (DP-BPSK), 56 Gbit/s (112 Gbit/s) QPSK (DP-QPSK), 84 Gbit/s (168 Gbit/s) 8PSK (DP-8PSK), and 112 Gbit/s (224 Gbit/s) 16QAM (DP-16QAM). For dual λ-channel (dual polarization) operation, the bitrates are 56 Gbit/s (112 Gbit/s) BPSK (DP-BPSK), 112 Gbit/s (224 Gbit/s) QPSK (DP-QPSK), 168 Gbit/s (336 Gbit/s) 8PSK (DP-8PSK), and 224 Gbit/s (448 Gbit/s) 16QAM (DP-16QAM).

All channels have equal average power. Each waveband ROADM is identically equipped with a variable optical attenuator (VOA) to mimic ROADM losses, an SOA under test, and a filter. The standard filter used is a 17 nm CWDM filter after each SOA. For the single λ-channel SP QPSK signal, we additionally investigate the two cases if a 2 nm filter or no filter is used. After the first, second and third waveband ROADM, the data signal is transmitted over 20 km, 20 km, and 10 km of standard single mode fiber (SMF).

We use four identical, commercially available SOAs (model CIP SOA-L-C-14-FCA) with 15 dB small signal fiber-to-fiber (FtF) gain (polarization dependency ± 0.3 dB) at 1550 nm (bias current 500 mA), 6.5 dB noise figure (NF, polarization dependency ± 0.3 dB), and a 1

#211942 - $15.00 USD Received 12 May 2014; revised 29 Jun 2014; accepted 30 Jun 2014; published 16 Jul 2014

dB saturation input power of −4 dBm. The representative FtF gain and NF for all four SOAs are shown in Fig. 3.

The total signal power into the first SOA is adjusted by the first VOA. All other VOAs are adjusted such that all SOAs have equal input power for a 0 dB net gain between subsequent SOA inputs. All SOAs have the same gain. The OMA input power is kept constant well above its sensitivity threshold for a bit error ratio (BER) of 10^{-9} for QPSK and 8PSK, and 10^{-6} for 16QAM. We analyze the error vector magnitude (EVM) [36] after each ROADM.

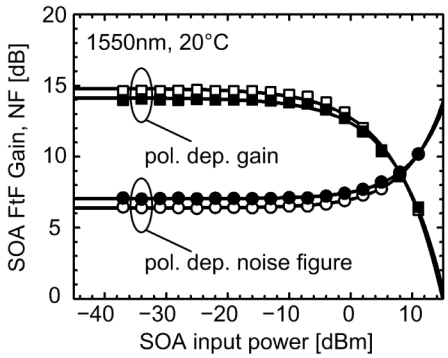

Fig. 3. Fiber-to-fiber (FtF) gain and noise figure (NF) of the SOAs used for the cascade experiment. All four SOAs have same characteristics. The 1 dB input saturation power is −4 dBm.

4. BER estimation from EVM for nonlinear amplification

In our experiment, we are interested in the IPDR along the SOA cascade. We define the IPDR as the ratio of the upper and lower SOA input power limits, inside which the EVM corresponds to a BER better than 10^{-3}. For instance, the vertical dashed lines in Fig. 4(a) indicate the upper and lower SOA input power limits for a single SOA amplifying a single λ-channel SP-QPSK signal (56 Gbit/s). The horizontal line indicates a BER of 10^{-3}. At low input powers the signal quality is limited by amplified spontaneous emission (ASE) noise. At high input power levels, the signal quality is limited by SOA nonlinearities.

The EVM is a performance measure for advanced modulation formats. Under the assumption of additive white Gaussian noise (AWGN), BER values can be accurately calculated from measured EVM values [36]. We measure EVM to judge the quality of our signal, because offline digital signal processing (DSP) and offline demodulation are used, which would make it very time consuming to reliably compute the BER. However, our definition of the IPDR is based on BER. Thus we first verify, for which SOA input power levels the assumption of AWGN is valid. We expect that the assumption does not hold in the nonlinear SOA regime.

Figure 4(b) compares actual measured BER values and BER values calculated from EVM measurements assuming AWGN for a single λ-channel SP-QPSK signal (56 Gbit/s). The signal was amplified by a single SOA. For a BER of 10^{-3}, the lower SOA input power limit obtained from actual measured BER values is only + 0.4 dB larger than the lower input power limit obtained from the BER values calculated from EVM measurements, i.e., EVM is quite a reliable metric for the lower input power limit. However, if the SOA amplifies nonlinearly, then the assumption of AWGN does not hold anymore. Then, the true upper power limit is smaller by −2 dB. In total, the true IPDR based on actual measured BER values is 2.4 dB smaller than the IPDR based on BER values which were calculated from EVM measurements. We did the same comparison for a single λ-channel SP-16QAM signal (112 Gbit/s). The deviation was + 0.5 dB for the lower input power limit and −2.6 dB for the upper input power limit. To account for this uncertainty, we subsequently subtract 3 dB from all IPDR values obtained from EVM measurements.

#211942 - $15.00 USD Received 12 May 2014; revised 29 Jun 2014; accepted 30 Jun 2014; published 16 Jul 2014

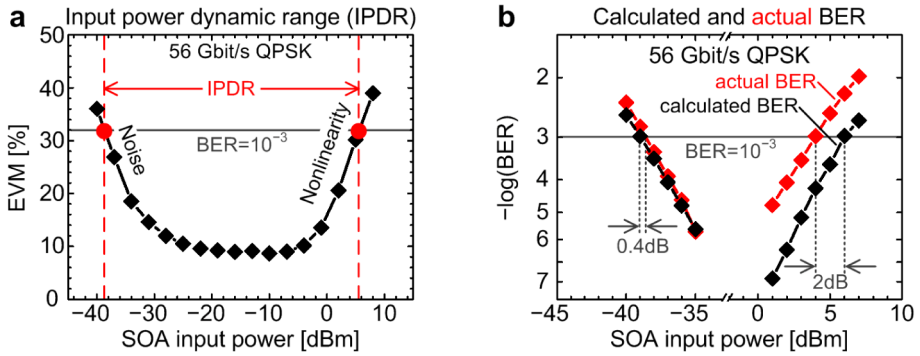

Fig. 4. (a) Error vector magnitude (EVM) as a function of the SOA input power and definition of the input power dynamic range (IPDR). The IPDR is defined as the ratio of the upper (nonlinearities) and lower (noise) SOA input power limits, inside which the EVM corresponds to a bit error ratio (BER) better than 10^{-3}. The upper and lower IPDR boundaries are indicated by the vertical dashed lines. (b) Relation between EVM and BER for low and large SOA input powers. Actual measured BER values and BER values calculated from EVM measurements assuming AWGN [36] are compared for QPSK.

5. Measurement results for advanced modulation formats in an SOA cascade

In this section, we discuss the EVM results obtained for the different modulation formats after each SOA along the cascade, if CWDM filtering is employed. For single λ-channel SP signals, we also analyze the phase and the magnitude error after each SOA. Furthermore, constellation diagrams are given to illustrate the limitations in the different operating regimes of the SOA. We also comment on the polarization dependence of the SOA cascade. From the measured EVM results in this section, we determine the IPDR for each modulation format along the SOA cascade. The summary of the IPDR results is then given in Section 6.

5.1 SOA cascade with BPSK signals

In Fig. 5, the SOA cascade results for BPSK modulation are shown. Figure 5(a) depicts the measured EVM after each of the four SOAs (SOA 1 black, SOA 2 red, SOA 3 green, SOA 4 blue) for single λ-channel (filled symbols) SP-BPSK as a function of the SOA input power. The solid horizontal line indicates the EVM limit corresponding to a BER of 10^{-3}. The dashed horizontal line indicates the back-to-back (BtB) signal quality without SOA cascade.

The associated constellation diagrams for the results given in Fig. 5(a) are shown in Fig. 5(g) for different SOA input power levels along the cascade. Additionally, we show in Fig. 5(b) the root-mean-square (rms) magnitude error (given as a percentage) and in Fig. 5(c) the rms phase error component (in degrees) of the EVM results of Fig. 5(a). The magnitude error is the difference in complex amplitude between the received symbol and the ideal constellation point normalized to the EVM normalization reference, which in our measurements is always the magnitude of the longest ideal constellation point. Knowing the different contributions of the magnitude error and the phase error to the overall EVM gives a more detailed insight by which mechanisms the signal is affected along the cascade.

At the best operating point with an input power of about −15 dBm (11 dB below the 1 dB gain saturation point) one finds a signal quality that is close to the BtB signal quality. At this operation point an SOA cascade with even more than four SOAs should work as well.

#211942 - $15.00 USD Received 12 May 2014; revised 29 Jun 2014; accepted 30 Jun 2014; published 16 Jul 2014

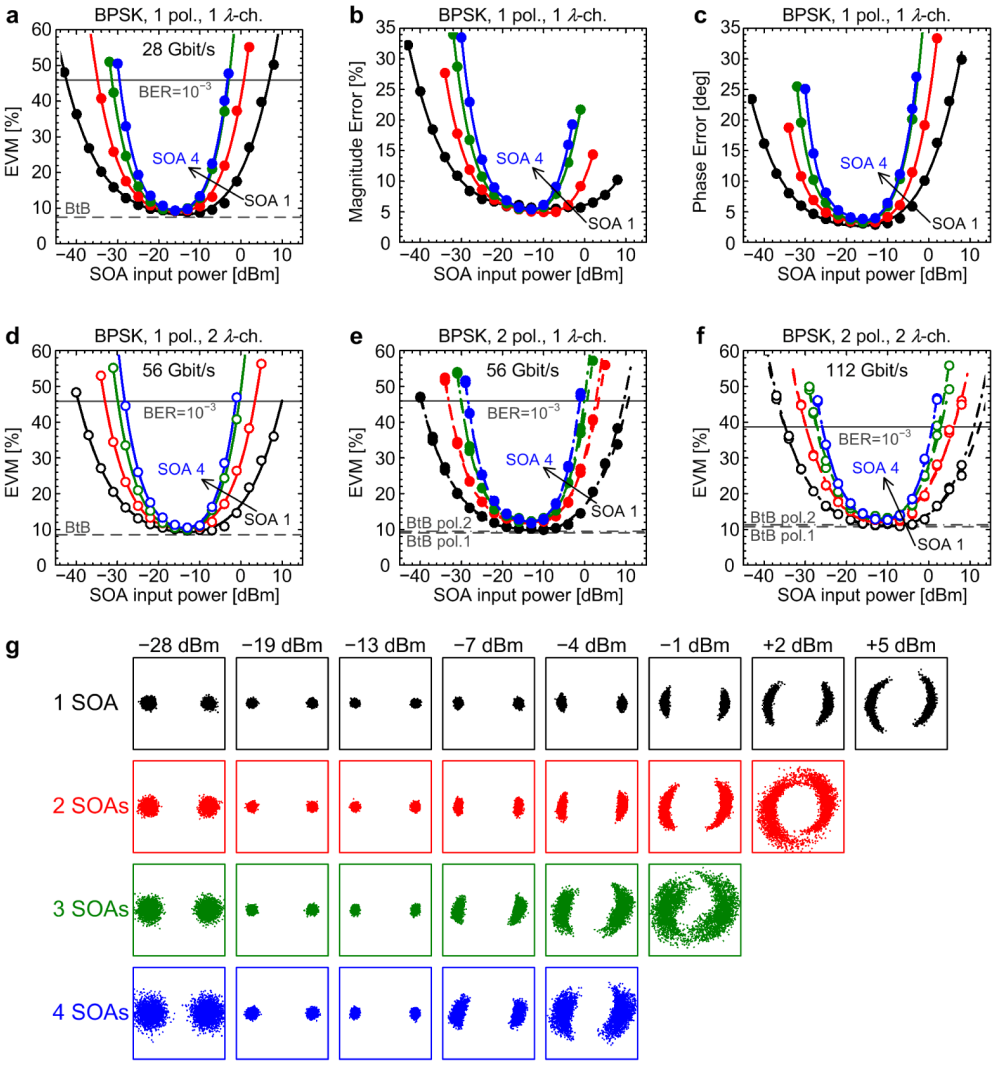

Fig. 5. EVM and constellation diagrams for BPSK signals in an SOA cascade. (a) EVM plot for the single λ-channel (filled symbols) single polarization (SP) signal, (b) magnitude error of the signal shown in (a), (c) phase error of the signal shown in (a). (g) Constellation diagrams of the single λ-channel SP constellation signal shown in (a) for different SOA input powers. (d) EVM plot of the dual λ-channel (open symbols) SP signal, (e) EVM plot of the single λ-channel dual polarization (DP, dashed and dash-dotted lines) signal, (f) EVM plot of the dual λ-channel DP signal. The solid horizontal lines indicate the EVM for a BER of 10^{-3}. Horizontal dashed/dash-dotted lines indicate the back-to-back (BtB) performance without SOAs.

For low input powers, the performance is limited by amplified spontaneous emission (ASE) noise, leading to a symmetric broadening of the constellation points (see Fig. 5(g) for −28 dBm). From Figs. 5(b) and 5(c) it can be seen that in this region both the magnitude errors and the phase errors contribute roughly equally to the overall EVM.

For large SOA input power levels, crescent-shaped constellations can be observed after the first SOA (see Fig. 5(g), first row, + 5 dBm). Figures 5(b) and 5(c) show that the dominating influence on EVM after the first SOA stems from phase errors. This is explained with zero-crossings of the field strength between symbols caused by the Tx used in this experiment [35]. The resulting gain change in the SOA then causes unwanted phase deviations by amplitude-phase coupling [26] leading to a crescent-shaped constellation.

#211942 - $15.00 USD Received 12 May 2014; revised 29 Jun 2014; accepted 30 Jun 2014; published 16 Jul 2014

By cascading several SOAs, nonlinear (NL) distortions and ASE noise accumulate. When looking at the constellation diagrams in Fig. 5(g) for small input powers, one can observe how the noise and the symmetric broadening of the constellation diagrams increase for an increasing number of SOAs. In saturation (see −1 dBm), the distinct crescent-shaped constellation diagram is getting broader, the more SOAs are cascaded. This fact is also observed in Fig. 5(b), where the magnitude error for large input power levels is significantly increased if the signal is amplified by more than one SOA. This effect can be understood by the NF of the SOA (see Fig. 3), which grows in saturation. This increase in NF is particularly unfavorable when several SOAs are cascaded.

Figure 5(d) depicts the measured EVM of one representative channel in the SP dual λ-channel operation (open symbols), where both λ-channels share the SOA gain. Since the total average SOA input power is depicted, the actual power per λ-channel is 3 dB lower, and hence the curves are shifted by about 3 dB to the right compared to single λ-channel operation, compare with Fig. 5(a). The same rules for the actual per-channel power apply also for the other modulation formats investigated in the following sections. The presence of a second λ-channel with a frequency spacing of 150 GHz to the first λ-channel shows no impairments. This is attributed to the almost continuous wave nature of phase-encoded signals. Thus one signal can be considered as a holding beam for the other signal [16]. The summary of IPDR values in Table 1 even indicates a slight increase in IPDR in the order of 1 dB for dual λ-channel BPSK and QPSK operation compared to single λ-channel operation.

Figures 5(e) and 5(f) show the EVM for DP operation (dashed and dash-dotted lines) in one λ-channel (e), and for one representative λ-channel in a dual λ-channel operation (f). The horizontal dashed and dash-dotted lines indicate the BtB results for both polarizations. For dual λ-channel and DP operation, four independent signals are amplified, thus the input power per channel is reduced by 6 dB. Virtually no degradation in signal quality is seen for DP operation compared to SP operation. These results suggest that SOA cascades with considerably more than four SOAs are possible for DP-BPSK signaling.

5.2 SOA cascade with QPSK and 8PSK signals

In analogy to the BPSK results presented in Fig. 5, the EVM results and constellation diagrams for QPSK and 8PSK are shown in Fig. 6 and Fig. 7, respectively. In general, the same statements which were made for BPSK also hold for QPSK and 8PSK. All the three formats BPSK, QPSK, and 8PSK are phase-modulated signals with only one amplitude level, and are limited by the same effects inside the SOA cascade. However, for QPSK and 8PSK the distance between neighboring constellation points is smaller compared to BPSK. Thus, noise and / or nonlinearities will limit the performance already at higher / lower input power levels compared to BPSK. Consequently, the IPDR for both QPSK and 8PSK will be smaller than for BPSK.

In Fig. 6(g) and Fig. 7(g), the constellation diagrams for single λ-channel SP-QPSK and SP-8PSK, respectively, show only little impairments after four cascaded SOAs at an input power of −13 dBm which is close to the optimum operation point of −15 dBm. The good signal quality can also be seen in Figs. 6(a), 6(d), 7(a), and 7(d) showing the measured EVM along the SOA cascade for the single λ-channel (a) and dual λ-channel (d) SP signals. From these measurements, we conclude that single λ-channel and dual λ-channel SP-QPSK / 8PSK signals may also be transmitted over more than four cascaded SOAs.

For DP-QPSK, one can see from Figs. 6(e) and 6(f) that after the third SOA (green), the performance of one polarization is slightly worse than the performance of the second polarization and also worse than the performance of both polarizations after the fourth SOA (blue). We attribute this irregularity to the interplay between the random state of polarization in the transport fiber and the slightly polarization-dependent gain (PDG) of the SOA. The effect of the PDG on the SOA cascade will be discussed later. For DP-8PSK signals, Figs. 7(e) and 7(f), the irregularities due to polarization issues are more pronounced than for DP-QPSK.

#211942 - $15.00 USD Received 12 May 2014; revised 29 Jun 2014; accepted 30 Jun 2014; published 16 Jul 2014

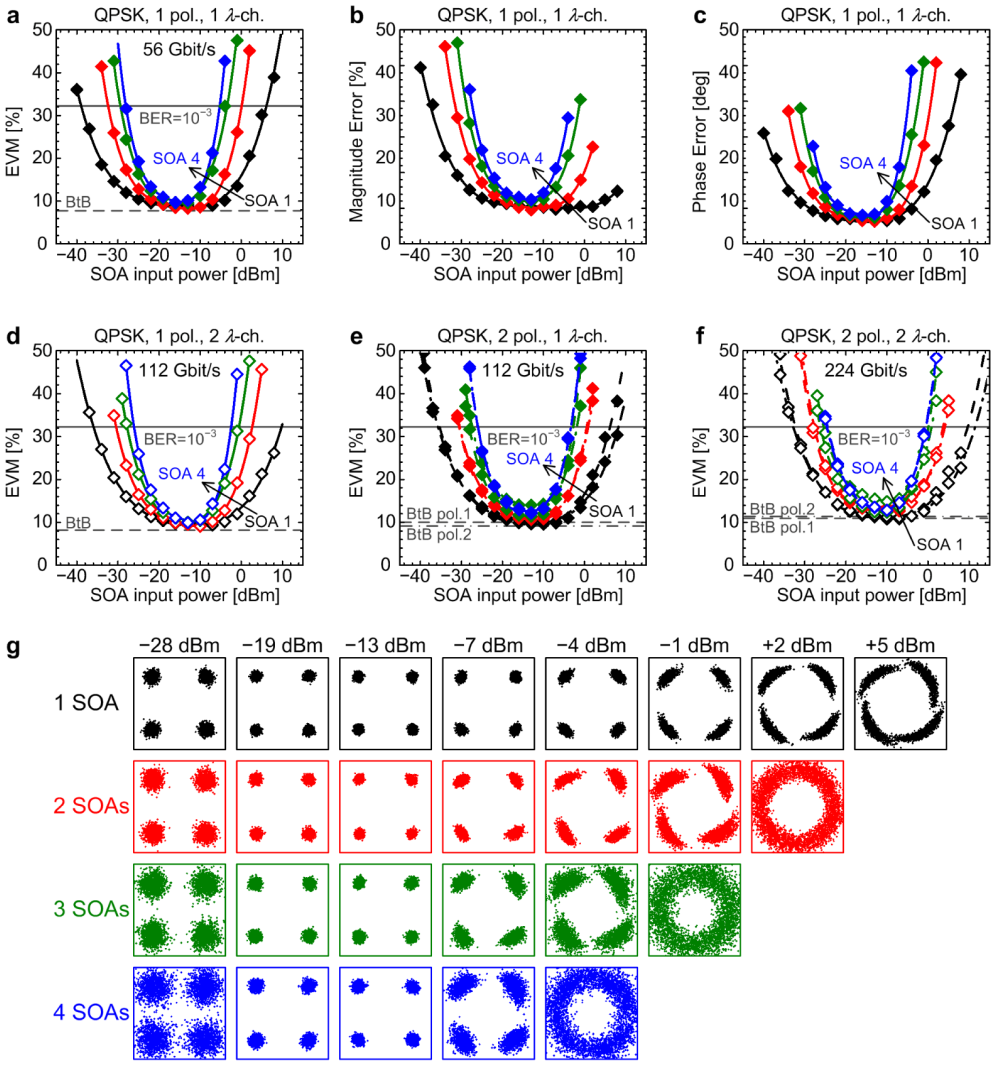

Fig. 6. EVM and constellation diagrams for QPSK signals in an SOA cascade. (a) EVM plot for the single λ-channel (filled symbols) single polarization (SP) signal, (b) magnitude error of the signal shown in (a), (c) phase error of the signal shown in (a). (g) Constellation diagrams of the single λ-channel SP constellation signal shown in (a) for different SOA input powers. (d) EVM plot of the dual λ-channel (open symbols) SP signal, (e) EVM plot of the single λ-channel dual polarization (DP, dashed and dash-dotted lines) signal, (f) EVM plot of the dual λ-channel DP signal. The solid horizontal lines indicate the EVM for a BER of 10^{-3}. Horizontal dashed/dash-dotted lines indicate the back-to-back (BtB) performance without SOAs.

#211942 - $15.00 USD Received 12 May 2014; revised 29 Jun 2014; accepted 30 Jun 2014; published 16 Jul 2014

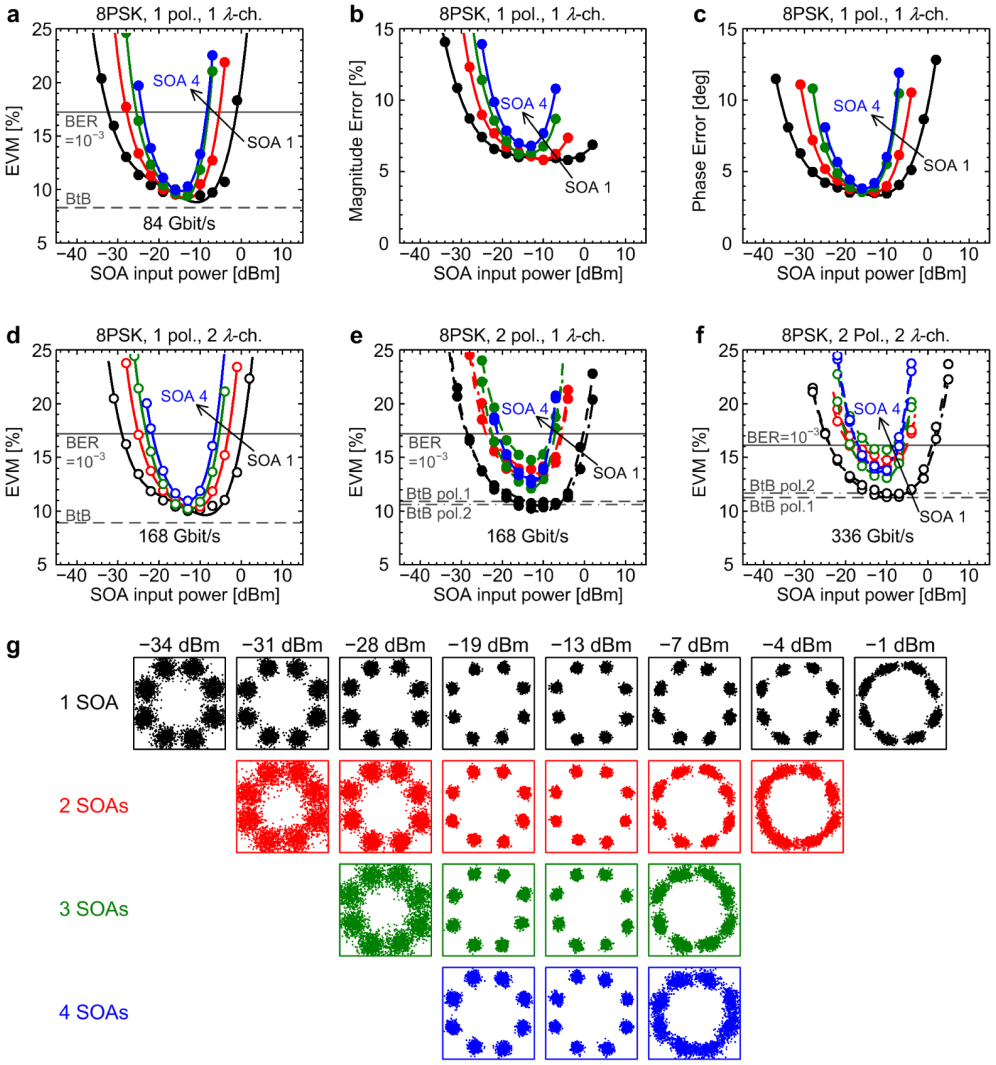

Fig. 7. EVM and constellation diagrams for 8PSK signals in an SOA cascade. (a) EVM plot for the single λ-channel (filled symbols) single polarization (SP) signal, (b) magnitude error of the signal shown in (a), (c) phase error of the signal shown in (a). (g) Constellation diagrams of the single λ-channel SP constellation signal shown in (a) for different SOA input powers. (d) EVM plot of the dual λ-channel (open symbols) SP signal, (e) EVM plot of the single λ-channel dual polarization (DP, dashed and dash-dotted lines) signal, (f) EVM plot of the dual λ-channel DP signal. The solid horizontal lines indicate the EVM for a BER of 10^{-3}. Horizontal dashed/dash-dotted lines indicate the back-to-back (BtB) performance without SOAs.

5.3 SOA cascade with 16QAM signals

The results for the 16QAM signals are shown in Fig. 8. At small SOA input powers, the performance is again limited by ASE noise. In saturation, magnitude errors significantly contribute to the EVM already after amplification by the first SOA, see Fig. 8(b). The largest amplitude level (outermost symbols) is compressed and becomes (almost) indistinguishable from the middle amplitude level, see constellations diagrams for input power levels > −10 dBm in Fig. 8(g). Due to the proximity of the symbols in the constellation diagram, the IPDR will further decrease compared to QPSK and 8PSK. However, as can be seen from Figs. 8(a) and 8(d)–8(f), around the optimum SOA cascade input power, an SOA cascade comprising

#211942 - $15.00 USD Received 12 May 2014; revised 29 Jun 2014; accepted 30 Jun 2014; published 16 Jul 2014

four SOAs is feasible. This enables high-capacity paths with data rates > 200 Gbit/s over 50 km SMF. However, irregularities due to polarization issues are seen for DP-16QAM in Figs. 8(e) and 8(f).

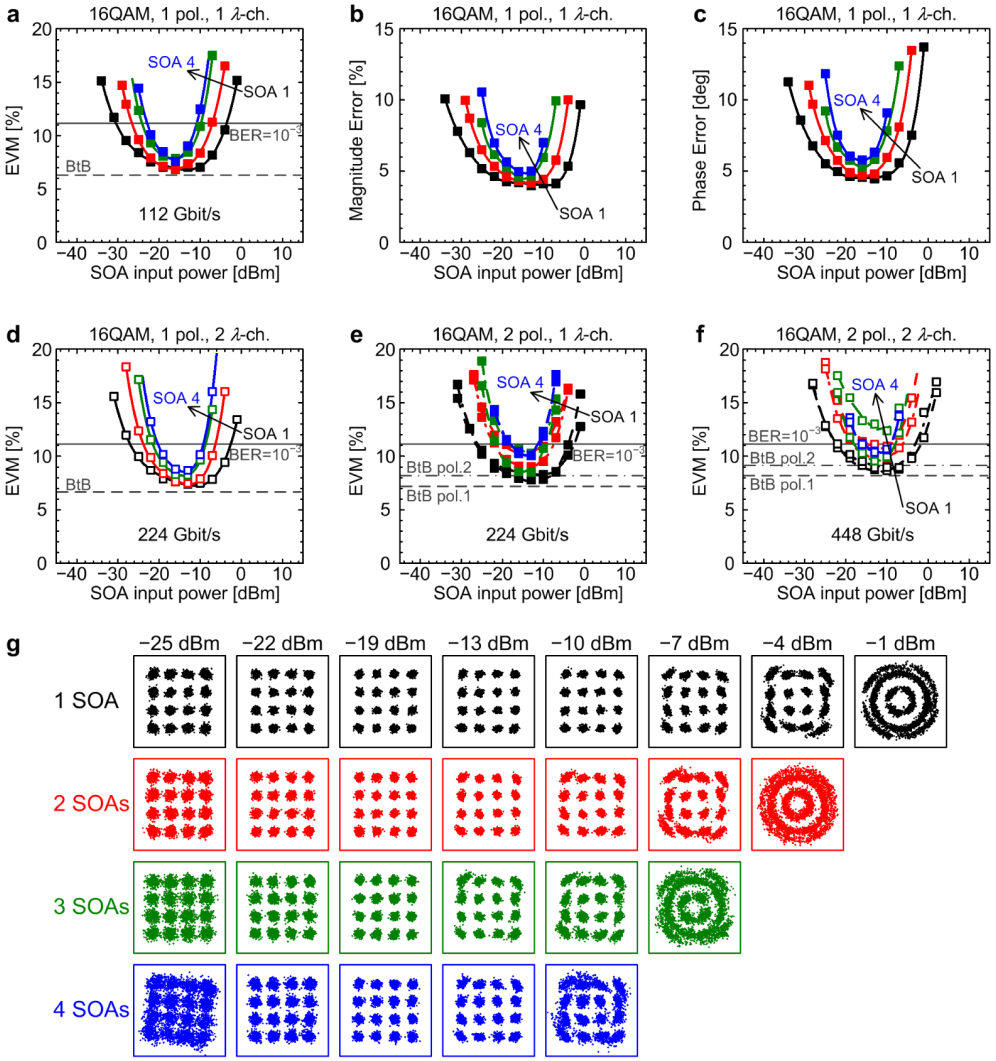

Fig. 8. EVM and constellation diagrams for 16QAM signals in an SOA cascade. (a) EVM plot for the single λ-channel (filled symbols) single polarization (SP) signal, (b) magnitude error of the signal shown in (a), (c) phase error of the signal shown in (a). (g) Constellation diagrams of the single λ-channel SP constellation signal shown in (a) for different SOA input powers. (d) EVM plot of the dual λ-channel (open symbols) SP signal, (e) EVM plot of the single λ-channel dual polarization (DP, dashed and dash-dotted lines) signal, (f) EVM plot of the dual λ-channel DP signal. The solid horizontal lines indicate the EVM for a BER of 10^{-3}. Horizontal dashed/dash-dotted lines indicate the back-to-back (BtB) performance without SOAs.

5.4 Optical spectra along the SOA cascade

The normalized spectra (resolution bandwidth RBW = 0.01 nm) after each SOA of the cascade for single λ-channel SP-QPSK and dual λ-channel SP-QPSK are shown in Figs. 9(a) and 9(b), respectively. The total SOA input power of the signals was $P_{SOA} = -13$ dBm (close to the optimum operation point of −15 dBm). Most of the ASE noise of the SOAs is filtered by a

#211942 - $15.00 USD Received 12 May 2014; revised 29 Jun 2014; accepted 30 Jun 2014; published 16 Jul 2014

CWDM filter. It can be seen how the ASE noise accumulates along the SOA cascade within the CWDM filter bandwidth. The tilt of the ASE noise floor results from the wavelength dependent SOA gain.

Figure 9(c) shows the normalized optical spectrum after the second SOA for dual λ-channel SP-QPSK for a total input power level of + 2 dBm (nonlinear regime) corresponding to a power of −1 dBm per λ-channel. Four-wave mixing (FWM) products can be seen 36 dB and 38 dB below the two channel peaks. These FWM products could deteriorate the signal quality in other λ-channels located at the same frequencies as the newly created FWM products. In practice, however, this is an unrealistic case, because the SOA cascade would not be operated at such large input powers where already a single λ-channel is severely distorted by amplitude-phase coupling as discussed before. The reason for signal degradation at low input powers, namely ASE noise accumulation, can be seen from the optical spectrum. However, for high input powers, the signal degrades primarily because of amplitude-phase coupling, and this cannot be seen from the spectrum. FWM products in the spectrum appear only at even larger input power levels.

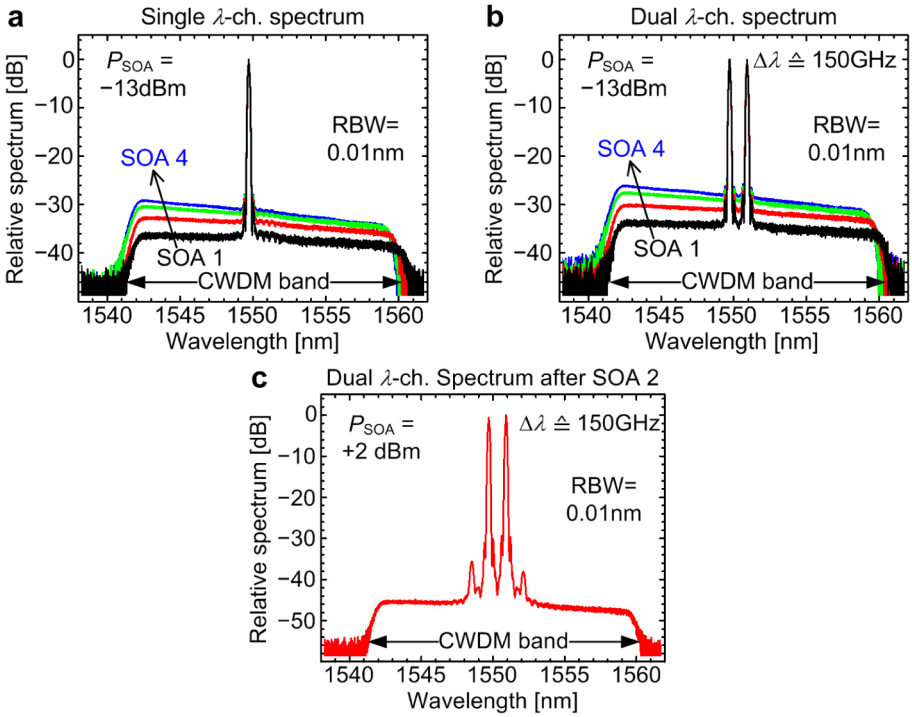

Fig. 9. Normalized optical spectra (resolution bandwidth RBW = 0.01 nm) along the SOA cascade for a total SOA input power of −13 dBm, (a) single λ-channel SP-QPSK, (b) dual λ-channel SP-QPSK. (c) Spectrum for dual λ-channel SP-QPSK signal after second SOA and a large total SOA input power of + 2 dBm. Four-wave-mixing products can be seen.

5.5 SOA cascade polarization dependence

An irregular performance of one polarization when amplifying DP signals, especially DP-16QAM, was observed and discussed previously. The irregularities are attributed to the interplay between the random state of polarization in the transport fiber and the slight PDG of the SOAs. By adjusting the input polarization at each SOA in the cascade to the minimum (maximum) gain, we evaluate the best (worst) case.

The effect of the PDG after one and four SOAs is depicted in Fig. 10(a) for a single λ-channel SP-QPSK signal and in Fig. 10(b) for a single λ-channel SP-16QAM signal. The up-

#211942 - $15.00 USD Received 12 May 2014; revised 29 Jun 2014; accepted 30 Jun 2014; published 16 Jul 2014

per power limit of the IPDR reduces by 2 to 3 dB, if the polarization is adjusted from minimum to maximum SOA gain.

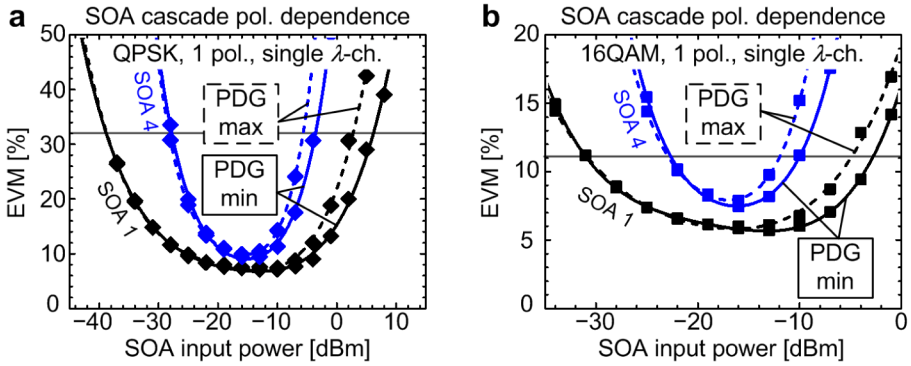

Fig. 10. Effect of polarization dependent gain (PDG) on SOA cascade. (a) single λ-channel SP-QPSK, (b) single λ-channel SP-16QAM. The upper power limit of the input power dynamic range (IPDR) reduces by 2 to 3 dB, if the polarization is adjusted from minimum to maximum SOA gain.

In our SOA cascade experiment, we did not use any polarization controllers at the SOA because such an element would not be practical in a real network implementation. Our experiments suggest that the combination of random polarization in the transport fiber and a cascade of several SOAs with each SOA having a polarization dependency of "only" ± 0.3 dB may lead to performance fluctuations and signal degradation. However, as we do not expect the PDG of SOAs to become much lower than ± 0.3 dB, more detailed investigations on polarization as a limiting factor are required for quantifying this kind of degradation.

6. IPDR of an SOA cascade with advanced modulation formats

This section discusses the IPDR results which were obtained from the EVM measurements in the previous section. The IPDR values for the different modulation formats transmitted over the SOA cascade are then summarized in a table. We also discuss the influence of different filter bandwidths after each SOA on the IPDR along the cascade. For this purpose we transmit the single λ-channel SP-QPSK signal when employing a 2 nm filter and no filter after each SOA. The results are compared with those obtained for the single λ-channel SP-QPSK signal when employing a CWDM filter.

6.1 IPDR results for SOA cascade with CWDM filters

As described in Section 4, all IPDR values are corrected (reduced) by 3 dB to account for the difference between the actual BER and the BER values calculated from the EVM measurements in the nonlinear SOA regime where the assumption of AWGN does not hold.

Figure 11(a) shows the IPDR as a function of the number of cascaded SOAs for SP signals. The IPDR results for DP signals are shown in Fig. 11(b) (polarization 1) and Fig. 11(c) (polarization 2), respectively. Single λ-channel results are represented by filled symbols, and dual λ-channel results are represented by open symbols.

Both SP-QPSK and DP-QPSK formats exhibit an excellent IPDR of 20 dB after four SOAs, indicating that a high-capacity path with > 100 Gbit/s over a fiber length of 50 km is feasible. The QPSK signal is very robust and may also be employed in SOA cascades with more than four SOAs. This is sufficient for most of the application scenarios in future converged metro-access networks. Single-polarization 8PSK (SP-8PSK) signals offer a good IPDR of 12 dB (10 dB) after four cascaded SOAs. With SP-16QAM, an acceptable IPDR of 8 dB after four concatenated SOAs indicates a functional path. DP-16QAM still works with a small IPDR of 4 dB after four SOAs. However, due to polarization-related issues, irregularities after the second and third SOA can be seen.

#211942 - $15.00 USD Received 12 May 2014; revised 29 Jun 2014; accepted 30 Jun 2014; published 16 Jul 2014

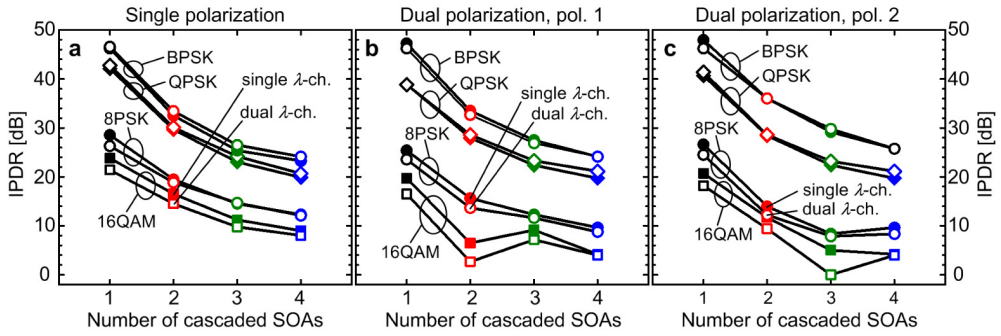

Fig. 11. Input power dynamic range (IPDR) as a function of the number of cascaded SOAs for (a) single polarization (SP) signals, (b) polarization 1 of dual polarization (DP) signals, (c) polarization 2 of DP signals. QPSK is a very robust signal. An IPDR of at least 20 dB is obtained after four SOAs. The DP-16QAM signals show some irregularities due to polarization dependent issues.

Table 1 summarizes all IPDR values obtained in our measurements over a cascade of up to four SOAs and with CWDM filtering after each SOA. The QPSK signals are found to be very robust and represent a good trade-off between capacity and reach. QPSK offers twice the capacity of traditional OOK, and a cascade with more than four SOAs and QPSK modulation is feasible. The use of 16QAM offers capacities of nearly half a Tbit/s. However, especially DP-16QAM is only recommended over shorter distances.

There is an IPDR trade-off between the modulation format that is used, which defines the capacity per channel, and the number of cascadable SOAs, which defines the distance that can be bridged in the ring network. In future access networks, resources can be allocated dynamically. For instance, a high-capacity path between two enterprises uses a single λ-channel with DP-QPSK modulation providing 112 Gbit/s capacity. On demand, this capacity can be increased to 224 Gbit/s either by adding another λ-channel with DP-QPSK modulation, or if a second λ-channel is not available, by changing the modulation format of the current λ-channel to DP-16QAM. Depending on the distance (number of ROADMs) between both enterprises, the IPDR could be insufficient for DP-16QAM. Then, a single λ-channel with DP-8PSK would be a possible trade-off providing a 168 Gbit/s capacity.

6.2 IPDR results for SOA cascade with 2 nm filters and no filters

To investigate the influence of the filter bandwidth after each SOA on the IPDR, we replace the 17 nm CWDM filters in the setup of Fig. 2 by 2 nm filters. In a second case, we do not use any post-SOA filter at all. We transmit the single λ-channel SP-QPSK signal and compare the IPDR results to the results obtained with CWDM filtering.

In Fig. 12, the normalized spectra (resolution bandwidth RBW = 0.01nm) after each SOA of the cascade are shown for the cases when no filter is employed, Fig. 12(a), and or if a 2 nm filter is used, Fig. 12(b) (compare to Fig. 9(a) for CWDM filtering). When no filter is used, Fig. 12(a), all the ASE noise of one SOA is passed to the next SOA in the cascade. For low SOA input powers, the ASE noise becomes a major part of the total signal power. The subsequent SOA in the cascade will amplify the large amount of ASE from the previous amplifier and add its own ASE noise. By employing a filter after each SOA, the out-of-band ASE noise can be significantly reduced, see Fig. 12(b). For the same SOA input power, the ASE noise portion of the total signal power is reduced compared to the case when no filter is employed. It should be noted that for all three filtering cases, always the same Rx with a 0.6 nm Rx filter is used. Thus, the difference between the three considered cases is the portion of ASE noise along the SOA cascade with respect to the total signal power. The question is, how much does the IPDR along the SOA cascade change (improve) as a function of the filter bandwidth used after each SOA?

#211942 - $15.00 USD Received 12 May 2014; revised 29 Jun 2014; accepted 30 Jun 2014; published 16 Jul 2014

Table 1. Summary of measured input power dynamic range (IPDR) values for a BER < 10^{-3} along a cascade of four identical SOAs when using advanced modulation formats, a 0 dB net gain between subsequent SOA inputs, and CWDM filtering after each SOA. The two numbers given for DP signals denote the IPDR of both polarizations. The color grading (see legend below the Table) gives a hint to identify possible operation conditions in the network.

Pol.	Modulation # of λ ch.	Format	IPDR after n-th SOA [dB] $n=1$	$n=2$	$n=3$	$n=4$	Data rate [Gbit/s]
Single Polarization (SP)	1	BPSK	46	33	25	23	28
	1	QPSK	42	30	23	20	56
	1	8PSK	29	19	15	12	84
	1	16QAM	24	17	11	9	112
	2	BPSK	47	33	27	24	56
	2	QPSK	43	30	24	21	112
	2	8PSK	26	19	15	12	168
	2	16QAM	21	15	10	8	224
Dual Polarization (DP)	1	BPSK	47 46	34 33	28 27	24 24	56
	1	QPSK	39 41	28 28	22 22	20 20	112
	1	8PSK	25 27	16 14	12 8	10 10	168
	1	16QAM	20 21	7 12	9 5	4 4	224
	2	BPSK	48 46	36 36	29 30	26 26	112
	2	QPSK	39 41	29 29	23 23	21 21	224
	2	8PSK	24 25	14 12	12 8	9 8	336
	2	16QAM	17 18	3 9	7 0	4 4	448
IPDR color map:			0…5 dB		6…19 dB		> 19 dB

Figure 13(a) depicts the upper and lower IPDR boundary (= upper and lower SOA input power limit) as a function of the number of cascaded SOA for the three different filter options (with-out filter, CWDM filter, 2 nm filter). It can be seen, that the upper IPDR boundary is virtually not affected by the filter bandwidth. The upper IPDR boundary is determined by nonlinear effects in the SOA. As expected, filtering has an influence on the lower IPDR boundary and thus on the achievable IPDR along the SOA cascade. For decreasing filter bandwidth (the measurement without filter represents the largest filter bandwidth) the lower IPDR boundary is shifting to lower SOA input powers, i.e. the IPDR is increasing. The quantitative effect of the different filter bandwidths on the IPDR along the SOA cascade is shown in Fig. 13(b). For the CWDM filter scheme, a 7 dB larger IPDR is achieved after the fourth SOA compared to the transmission without filter. For a filter bandwidth of 2 nm, the IPDR is 11 dB larger after the fourth SOA compared to the case without filter.

#211942 - $15.00 USD Received 12 May 2014; revised 29 Jun 2014; accepted 30 Jun 2014; published 16 Jul 2014

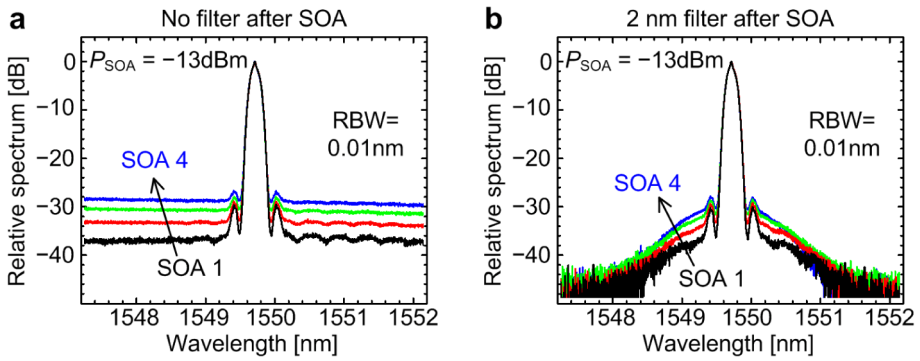

Fig. 12. Normalized optical spectra (resolution bandwidth RBW = 0.01 nm) for single λ-channel SP-QPSK along the SOA cascade. (a) Without filter after each SOA, (b) with a 2 nm filter after each SOA. The total SOA input power is −13 dBm.

It should be pointed out that the use of a 2 nm filter would rather aim on filtering a single channel or an individual subchannel within a wavelength band, e.g., a CWDM wavelength band. However, this would considerably increase the waveband ROADM complexity. As demonstrated with our experiments, already the use of only CWDM filters considerably improves the IPDR along the SOA cascade. Table 2 summarizes the IPDR results for different filter bandwidths.

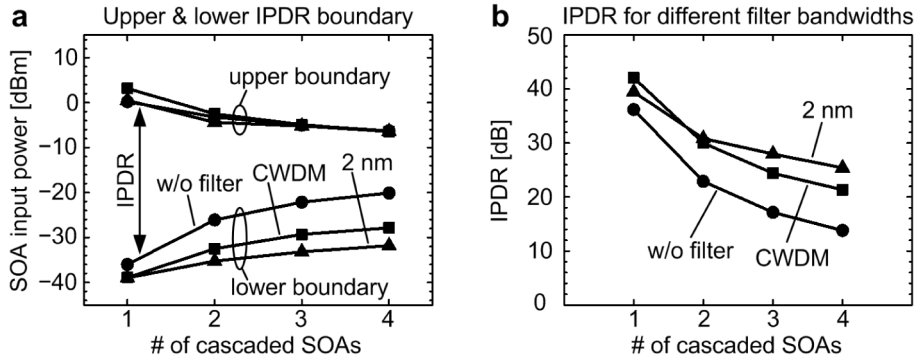

Fig. 13. (a) Upper and lower boundary of the input power dynamic range (IPDR) as a function of the number of cascaded SOAs for different filter bandwidths (no filter, 17 nm CWDM filter, 2 nm filter). (b) IPDR as a function of the number of cascaded SOAs. By employing CWDM filters along the SOA cascade, the IPDR after the fourth SOA is increased by 7 dB compared to the case without filter.

Table 2. Influence of different filter bandwidths on the input power dynamic range (IPDR) along a cascade of four identical SOAs with single λ-channel SP-QPSK and a 0 dB net gain between subsequent SOA inputs. The use of a CWDM filter gives a 7 dB larger IPDR after four SOAs compared to the case if no filter is used.

Single λ-channel SP-QPSK Filter after each SOA	IPDR after n-th SOA [dB] $n = 1$	$n = 2$	$n = 3$	$n = 4$	Data rate [Gbit/s]
No filter	36	23	17	14	56
17 nm filter (CWDM)	42	30	24	21	56
2 nm filter	39	31	28	25	56
IPDR color map:	0…5 dB		6…19 dB		> 19 dB

7. Conclusions

In this paper, we demonstrate that signals encoded with advanced modulation formats such as BPSK, QPSK, 8PSK, and 16QAM can be amplified by at least four cascaded SOAs. This

#211942 - $15.00 USD Received 12 May 2014; revised 29 Jun 2014; accepted 30 Jun 2014; published 16 Jul 2014

enables high-capacity paths with a high data capacity in the order of a Tbit/s for future converged metro-access ring networks.

A large IPDR of > 20 dB is found for SP-QPSK and DP-QPSK signals after four cascaded SOAs, indicating that even a larger number of SOAs can be cascaded. With SP-8PSK and DP-8PSK, an acceptable IPDR of about 10 dB after four cascaded is achieved. Also the demanding 16QAM signals can be transmitted over four SOAs, after all with an IPDR of 4…8 dB. Thus, the robust QPSK signal is recommended for large transmission distances. More complex formats are a viable option for very large capacities over shorter distances.

Despite the small PDG of ± 0.3 dB of the SOAs used in this paper, our experiments show irregular performance of one polarization when amplifying DP signals, especially for DP-16QAM. This is attributed to the interplay between the random state of polarization in the transport fiber and the slightly polarization-dependent SOA gain. We recommend the usage of SOAs having the smallest possible polarization dependence of the gain.

The best SOA performance is found at input powers 11 dB below the 1 dB input saturation power, indicating that only linear SOAs can be used. For low input powers, the performance is limited by the accumulation of ASE noise along the SOA cascade. Thus, SOAs with a low noise figure are desirable to enlarge the achievable IPDR at the low input power side.

For phase-modulated signals (BPSK, QPSK, and 8PSK) the limitations after the first SOA (if operated in the nonlinear region) mainly result from amplitude-phase coupling. Gain changes during zero-crossing field strength transitions induce phase errors. For 16QAM, large amplitude changes are less likely. However, the SOA gain compression leads to the compression of the higher amplitude levels (magnitude errors). After more than one SOA, also the phase modulated signals suffer more and more from magnitude errors for large input power levels. The additional magnitude errors were attributed to the increasing NF of the SOA in saturation, and to the effect of cascading several SOAs which are all operated in their nonlinear regime. For an increasing number of SOAs, the upper and lower input power limit come closer and thus the IPDR decreases.

The dual λ-channel transmission experiments reveal only little signal quality impairments compared to the single λ-channel transmission experiments. We believe that due to the relatively weak amplitude variation for the investigated advanced phase modulation formats the amplification of such signals is almost comparable to the amplification of continuous wave signals. Both channels are amplified independently, and degradations due to inter-channel cross-talk (cross-gain and cross-phase modulation) are weak. This is in contrast to the amplification of multi-channel OOK signals, where inter-channel crosstalk is a major issue in SOA saturation.

Semiconductor optical amplifiers offer a large gain bandwidth. Filtering after each SOA in an SOA cascade is beneficial to reduce unwanted out-of-band noise. We show that already the use of a CWDM filter (17 nm bandwidth) after each SOA enhances the IPDR by 7 dB after the fourth SOA compared to the case when no filter is used. When using a 2 nm filter bandwidth after each SOA, the IPDR after the fourth SOA increases by another 4 dB compared to the CWDM filter case.

Acknowledgments

This work was supported by the Karlsruhe School of Optics & Photonics (KSOP), by the CONDOR project (Converged Heterogeneous Metro/Access Infrastructure) funded by the German Federal Ministry of Research and Education (BMBF; grant 01BP1015), and the Agilent University Relations Program. We acknowledge support by Deutsche Forschungsgemeinschaft and Open Access Publishing Fund of Karlsruhe Institute of Technology.

#211942 - $15.00 USD Received 12 May 2014; revised 29 Jun 2014; accepted 30 Jun 2014; published 16 Jul 2014